RESEARCH ARTICLE | SEPTEMBER 03 2024

Femtosecond laser writing of durable open microfluidic channels via a mode-switchable strategy

Yahui Su; Linfeng Zheng; Zhaoxin Lao ; Zehang Cui; Chao Chen ; Chenchu Zhang ; Deng Pan; Yanlei Hu ; Sizhu Wu ; Yachao Zhang ; Dong Wu

Appl. Phys. Lett. 125, 101602 (2024)
https://doi.org/10.1063/5.0221736

Applied Physics Letters ARTICLE pubs.aip.org/aip/apl

Femtosecond laser writing of durable open microfluidic channels via a mode-switchable strategy

Cite as: Appl. Phys. Lett. **125**, 101602 (2024); doi: 10.1063/5.0221736
Submitted: 3 June 2024 · Accepted: 6 August 2024 ·
Published Online: 3 September 2024

Yahui Su,[1] Linfeng Zheng,[1] Zhaoxin Lao,[2] Zehang Cui,[3] Chao Chen,[4] Chenchu Zhang,[5] Deng Pan,[1] Yanlei Hu,[3] Sizhu Wu,[2,a)] Yachao Zhang,[2,a)] and Dong Wu[3]

AFFILIATIONS

[1]Information Materials and Intelligent Sensing Laboratory of Anhui Province, School of Electronics and Information Engineering, Anhui University, Hefei 230039, China
[2]Anhui Province Key Laboratory of Measuring Theory and Precision Instrument, School of Instrument Science and Optoelectronics Engineering, Hefei University of Technology, Hefei 230009, China
[3]CAS Key Laboratory of Mechanical Behavior and Design of Materials, Department of Precision Machinery and Precision Instrumentation, University of Science and Technology of China, Hefei 230027, China
[4]Department of Materials Physics and New Energy Device, School of Materials Science and Engineering, Hefei University of Technology, Hefei 230009, China
[5]Institute of Industry and Equipment Technology, Hefei University of Technology, Hefei 230009, China

[a)]**Authors to whom correspondence should be addressed:** sizhuwu@hfut.edu.cn and zyachao@hfut.edu.cn

ABSTRACT

Open microfluidic systems offer significant advantages, including the elimination of external pumps and facilitating fluid access at any point along the channel. However, their deployment in harsh environments is commonly compromised due to the delicate nature of hydrophilic chemical coatings and the vulnerability of open microchannels to clogging and contamination. Here, a bioinspired, demand-responsive mode-switchable strategy is proposed to enhance the mechanical durability of open microfluidic systems. Specifically, under harsh conditions or when long-term storage is necessary, this strategy allows the open microfluidic device to transition to a protective mode simply through releasing the strain, thereby preserving the integrity of the structure and hydrophilic coatings. The stretched open microfluidic mode enables spontaneous liquid spreading along a hydrophilic microchannel scribed by femtosecond laser. This mode-switchable strategy provides the open microfluidic device with robustness to maintain spontaneous liquid flow, even under severe testing conditions such as 2000 cycles of cotton swab rubbing, sand impact, sandpaper abrasion, tape peeling, twisting, and finger rubbing. A proof-of-concept application involving blood type analysis on this mode-switchable open microfluidic device showcases its superior mechanical durability under severe environmental conditions. The proposed strategy paves the way for the broader use of open microfluidic devices in various practical applications.

Point-of-care testing (POCT) is essential for early, noninvasive detection and diagnosis of diseases, particularly within developing areas or under conditions where resources are scarce.[1–3] Its foremost benefit lies in its ability to deliver quick and efficient testing outcomes, significantly reducing the wait for results.[4,5] Among various technologies, microfluidic devices stand out as particularly suitable for POCT owing to their distinct features, including minimal reagent usage, quick response, compact design, ease of production, and mobility.[6–10] Over the past decade, open microfluidic capillary systems have garnered widespread interest among researchers for their ability to operate without an external pump and their facilitation of easy sample access, allowing for fluid sampling or addition at any point along the channel.[11–16] This independence and accessibility afford open microfluidic systems a distinct advantage for a variety of applications including cell signaling studies,[13,17,18] microscale chemical reactions,[19,20] blood separation and analysis,[21,22] and glucose detection.[23,24]

However, current open microfluidic systems encounter two significant challenges that adversely affect their longevity in practical applications (Fig. 1). (1) Hydrophilic coatings lack mechanical durability, making them susceptible to wear and impairing the spontaneous

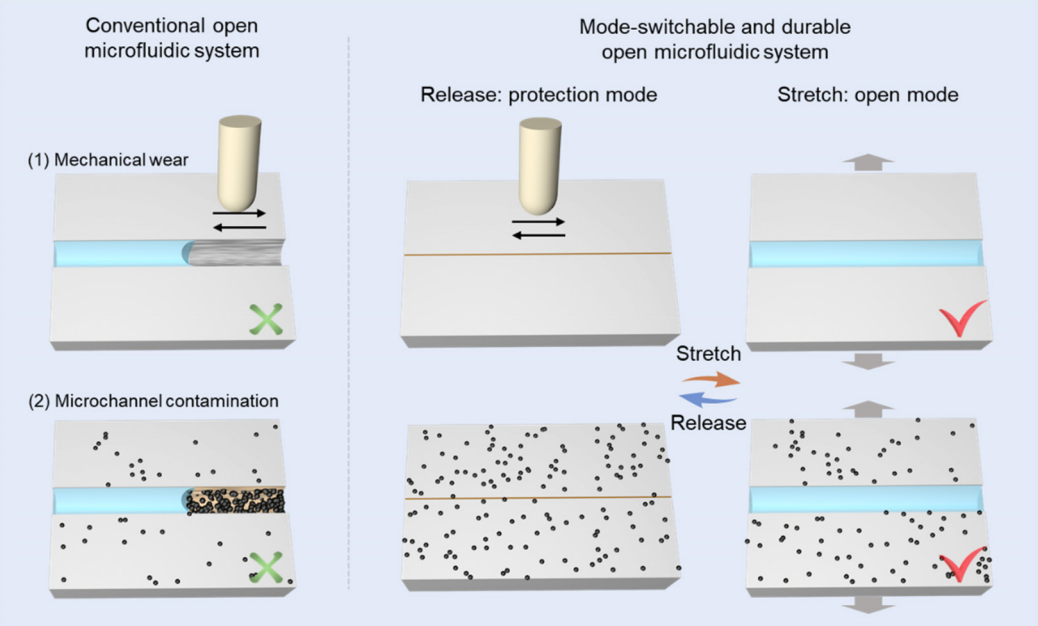

FIG. 1. Comparison of conventional and mode-switchable open microfluidic channels. Conventional open microfluidic systems encounter two significant challenges: (1) Hydrophilic coatings lack mechanical durability, making them susceptible to wear and impairing the spontaneous flow of fluids. (2) When the open microfluidic system is in a nonworking state, which constitutes the majority of its life cycle, the open channels are prone to blockage and contamination by dust particles from the environment. For the mode-switchable open microfluidic channels, the protection mode is specifically engineered to shield the microchannels and hydrophilic coatings from external abrasion and particulate blockages. This protection is achieved through simple release of the silicone membrane, which causes the microchannel to contract and seal within the membrane, thus preserving both the structural integrity and hydrophilic coatings.

flow of fluids.[25,26] (2) When the open microfluidic system is in a nonworking state, which constitutes the majority of its life cycle, the open channels are prone to blockage and contamination by dust particles from the environment.[27,28] Despite significant advancements in open microfluidic systems, the issue of durability has received insufficient attention. Therefore, developing a method to enhance the mechanical durability of open microfluidic systems is crucial for their practical applications.

Femtosecond laser processing stands out for its exceptional precision, minimal thermal impact, and mask-free flexibility, enabling the creation of open microfluidic systems on diverse materials with unmatched ease and efficiency.[29–31] For instance, Guo *et al.*[32] utilized femtosecond laser direct writing to develop a flexible method for creating self-driven microfluidic SERS silicon chips, enabling precise quantitative analysis of Hg^{2+} without the need for an external driving force and offering adjustable sample flow speeds through controlled channel properties. Yong *et al.*[33] employed a femtosecond laser to create superhydrophobic microchannels and microholes on PTFE surfaces for underwater gas self-transportation, demonstrating significant potential for innovative underwater gas manipulation applications.

Here, we propose a bioinspired mode-switchable strategy that allows for an on-demand transition between an active open microfluidic mode and a protective mode to address the aforementioned challenges. A hydrophilic open microchannel is fabricated on a uniaxially prestretched silicone membrane using femtosecond laser microfabrication, followed by treatment with a hydrophilicity-enhancing reagent. In the active open microfluidic mode, fluid movement is driven by capillary forces, enabling spontaneous flow. Drawing inspiration from the natural defense mechanism of a tortoise retracting into its shell in the face of danger, the protection mode is specifically engineered to shield the microchannels and hydrophilic coatings of the nonworking device from external abrasion and particulate blockages (Fig. 1). This protection is achieved through the simple release of the silicone membrane, which causes the microchannel to contract and seal within the membrane, thus preserving both the structural integrity and hydrophilic coatings. In this manner, the device demonstrates remarkable resistance against a series of stringent durability tests, including cotton swab rubbing, sand impacting, sandpaper abrasion, tape peeling, twisting, and finger rubbing, while maintaining spontaneous fluid transport upon restretching. Remarkably, the device maintains functionality even after 2000 cycles of cotton swab rubbing. A proof-of-concept application demonstrates blood type analysis using the device, which has undergone a series of stringent tests, demonstrating its mechanical durability under severe environmental conditions. This work offers helpful insights into the development of durable open microfluidic devices for practical applications.

Silicone exhibits advantages such as stretchability, wear resistance, and chemical stability, making it suitable as a substrate for fabricating microfluidic channels.[34–36] The femtosecond laser, with its noncontact nature, high processing precision, and flexibility, serves as a powerful tool for material processing. The manufacturing process of the durable open microfluidic channels is illustrated in Fig. 2(a). First, a silicone membrane (~2 mm thick) is cut into strips ($25 \times 75\ mm^2$), which are then uniaxially stretched. The strain value (ε) is defined by

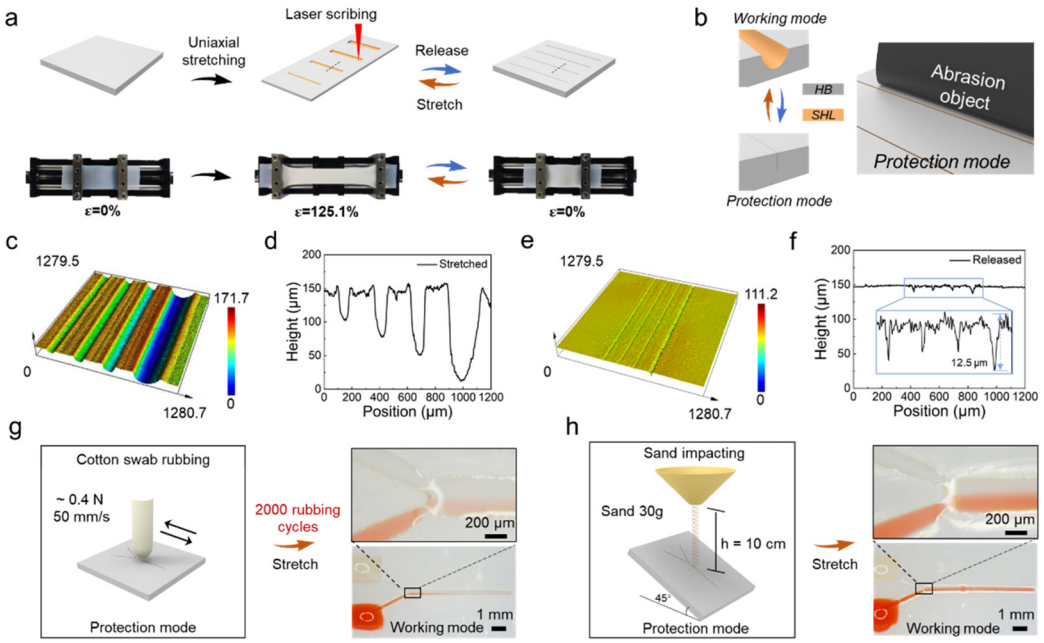

FIG. 2. Design and fabrication of a durable open microfluidic device. (a) Schematic and experimental images of femtosecond laser scribing open microchannels on a uniaxially stretched silicone membrane; ε is the strain applied to the membrane. (b) A cross-sectional schematic illustration showing the switching of the microchannel in (a) between the stretched open mode for operation and the release protection mode to defend against external abrasion. HB: hydrophobic. SHL: superhydrophilic. (c) Confocal laser scanning microscopy (CLSM) image of four microchannels fabricated with laser scribing for 7, 10, 13, and 16 cycles in stretched mode. (d) Cross-sectional profiles of the microchannels depicted in (c). (e) CLSM image of the same four microchannels in (c) but in release protection mode. (f) The cross-sectional profiles of the microchannels in (e), highlighting the reduced maximum depth of the channel to 12.5 μm in protection mode. (g) In protection mode, the open "Y"-shaped channels can resist 2000 cycles of cotton swab rubbing and (h) continuous sand impacting, effectively preserving the microfluid mixing function in stretched mode. One inlet introduces water, while the other introduces water dyed red, illustrating mixing capabilities.

the length of the film in its stretched (L) and initial (L_0) states, according to the equation $\varepsilon = (L - L_0)/L_0$. The laser is focused on the silicone surface, and microchannels are fabricated by scribing along a predefined path. Subsequently, a hydrophilic agent (polyethylene glycol solution) is sprayed onto the surface of the microchannels to achieve hydrophilicity.[36] To withstand mechanical wear and impact, the silicone membrane is switched to a protection mode through simple release of strain [Fig. 2(b)]. In the protection mode, the microchannels become completely sealed. During durability tests, the matrix material functions as a "soft armor" against mechanical abrasion and impact, effectively preserving the hydrophilic coating and microstructures. Using a femtosecond laser to ablate the membrane with 7, 10, 13, and 16 scribing cycles, four microchannels are fabricated with depths increasing from 46 to 138 μm and widths increasing from 92.5 to 251.25 μm. Their three-dimensional morphology and cross-sectional profiles are shown in Figs. 2(c) and 2(d). After releasing the strain to zero, the microchannels are closed, and their maximum depth is reduced to only 12.5 μm, indicating that the majority of the microchannel is concealed within the substrate material. In contrast, in the release state, four microchannels are fabricated using the same processing parameters with the femtosecond laser, where the groove depth increases from 6.7 to 14 μm, and the width remains at approximately 40 μm. Impressively, the protection mode can withstand 2000 cycles of cotton swab rubbing and continuous impact from 30 g of sand, effectively maintaining the microfluid mixing function through "Y" microchannels (7.5 mm in length) in the working mode [Figs. 2(g) and 2(h)]. In comparison, traditional open microfluidic channels can only withstand being rubbed with cotton swab for 200 cycles, and further rubbing results in the failure of fluid flow and mixing functions (Fig. S1 and supplementary Movie 1). In the sand impacting test, microchannels are blocked by small particles, not only increasing the fluid flow time through the entire channel from 1 to 8 s but also contaminating the fluid (Fig. S1 and supplementary Movie 2). Therefore, through the simple application and release of strain in the silicone, a switch between the working mode and protection mode is achieved, thus endowing the microchannels with durability without compromising the advantages of the open design.

By altering the laser processing parameters, the microchannel morphology can be regulated in a controlled manner. With the laser power and scribing speed fixed, an array of microchannel structures is fabricated by varying the number of laser scribing cycles (LSC, Fig. S2). Confocal laser scanning microscopy (CLSM) images of the three-dimensional morphology for one and nineteen laser scribing cycles are shown in Figs. 3(a) and 3(b), respectively. By extracting the cross-sectional profiles from laser confocal images, a series of microchannel profiles is obtained, as shown in Fig. 3(c). As the number of laser scribing cycles increases from one to nineteen, the groove depth increases from 5 to 124 μm [Fig. 3(e)], while the groove width increases from 17 to 105 μm before stabilizing [Fig. 3(f)], with the period remaining stable at approximately 285 μm [Fig. 3(g)]. The results indicate that

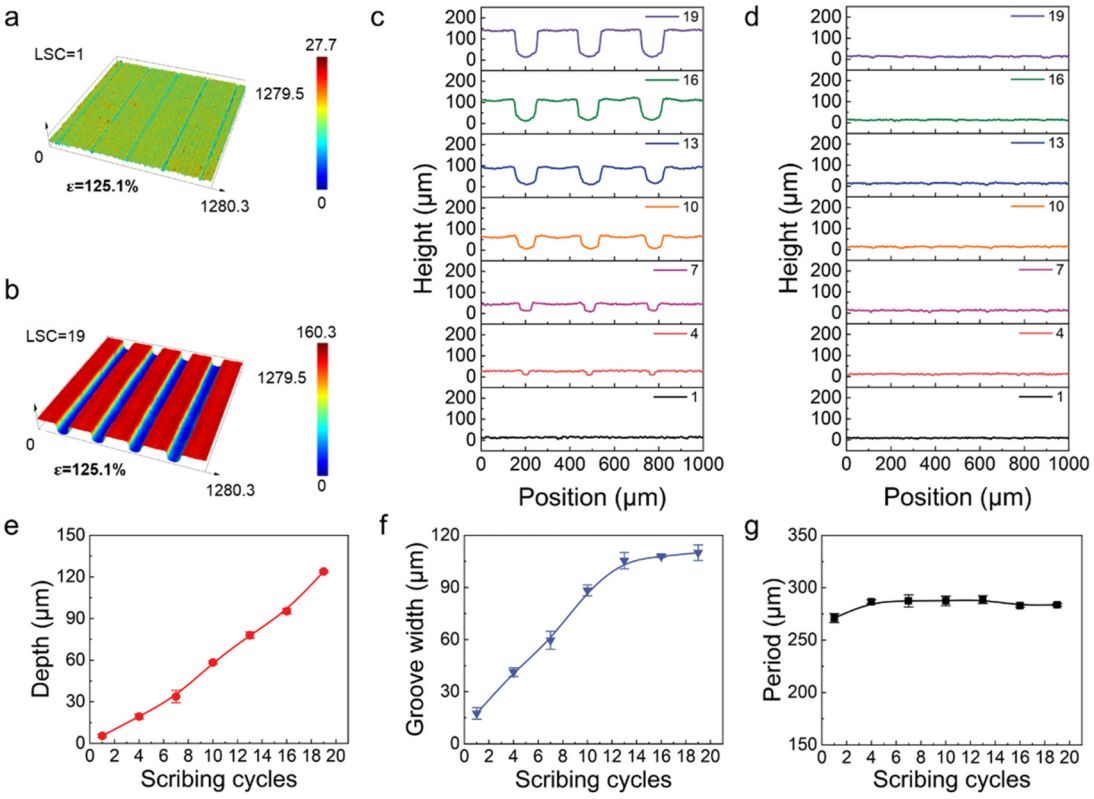

FIG. 3. Regulation of the open microchannel morphology by varying the number of laser scribing cycles. (a) CLSM image of microchannels fabricated with 1 cycle of laser scribing in the stretched mode. (b) CLSM image of microchannels fabricated with 19 cycles of laser scribing in the stretched mode. (c) Cross-sectional profiles of channels fabricated with increasing laser scribing cycles from 1 to 19 in the stretched mode. (d) The corresponding cross-sectional profiles of the channels in (c) but in the release mode. Variations in the depth (e), width (f), and period (g) of the channels with the number of laser scribing cycles from 1 to 19 in the stretched mode, demonstrating that precise control of the channel morphology can be achieved by changing the laser processing parameters.

increasing the number of scribing cycles yields wider and deeper grooves. Upon releasing the strain to zero, the corresponding CLSM images and profiles are shown in Fig. S3 and Fig. 3(d), respectively. The results demonstrate that microchannels at various depths can close well after the strain is released. When the aspect ratio of the microchannel exceeds a certain threshold, the microchannel becomes more prone to deformation under significant stress (Fig. S4). Therefore, the laser processing parameters need to be optimized to achieve precise fabrication of microchannels with consistent sizes.

The morphology of microchannels can also be tuned by adjusting the applied strain. Here, an array of microchannels is fabricated by laser scribing for 13 cycles. The three-dimensional morphology and cross-sectional profile of the microchannels under different strains are recorded using a laser confocal microscope. As shown in Figures 4(a)–4(c) and Fig. S5, the grooves gradually close and eventually become nearly invisible as the strain decreases from 125.1% to 7.8%. The reduction in strain leads to controllable contraction of the microchannels, with the cross-sectional profiles of the grooves transitioning from an initial "U" shape to a "V" shape, and finally the microchannels are completely closed [Fig. 4(d)]. Specifically, as the strain decreases from 125.1% to 7.8%, the depths of the grooves remain relatively unchanged (approximately 85 μm, between 62.1% and 125.1%), before gradually decreasing to 10 μm [Fig. 4(e)]; the widths of the grooves decrease from 121 to 17 μm [Fig. 4(f)], and the periods decrease from 297 to 69 μm [Fig. 4(g)]. Additionally, cyclic stretching and releasing tests with a strain range of 0%–125.1% are conducted [Fig. 4(h)]. The results show that the microchannel structure size under a strain of 125.1% changes very little after up to 20 cycles of stretching and releasing, demonstrating the durability and adaptability of the microchannel structure under repeated mechanical stress.

Before the durability tests, the impacts of water-soluble hydrophilic coating consumption and continuous stretch–release of the membrane on the liquid spreading time throughout the channel are investigated. Droplets are sequentially added to hydrophilically modified channels, and the spreading time is measured, ensuring that the liquid fully evaporates before proceeding to the next experiment. The spreading time increases with the number of droplet additions, indicating consumption of the hydrophilic coating (Fig. S6). Furthermore, the membrane undergoes nine cycles of stretching and releasing, and the droplets are added to the channel to measure the spreading time after the first, third, fifth, seventh, and nineth cycles. The increasing trend of the spreading time is consistent with that of the coating consumption experiments, suggesting that the cyclic stretch–release of the membrane does not affect the liquid flow (Fig. S6). Furthermore, the

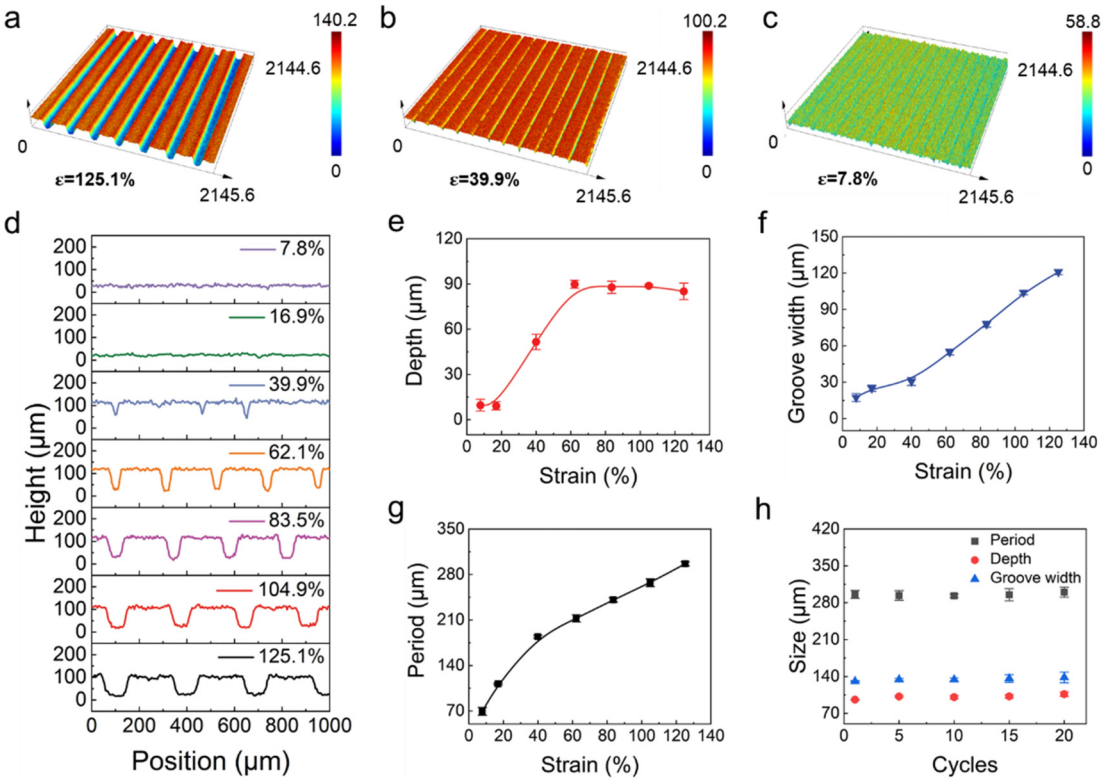

FIG. 4. Regulation of the morphology of open microchannels by varying the strain applied to the membrane. (a) CLSM image of microchannels fabricated with 13 cycles of laser scribing in the stretched mode under a strain of 125.1%. The same microchannels at strains of 39.9% (b) and 7.8% (c). (d) Cross-sectional profiles of the same microchannels under varying strains from 125.1% to 7.8%. Variations in the depth (e), width (f), and period (g) of channels with different strains from 125.1% to 7.8%, demonstrating the precise control over channel morphology enabled by adjusting the applied strain on the membrane. (h) Variations in the period, depth, and width of the microchannel across 20 cycles of membrane stretching and releasing.

influence of the prestretching strain applied on the membrane to the morphology of the microchannels in both stretched and released states is investigated (Fig. S7). Three microchannels are fabricated on silicone membranes at strains of 125.1%, 62.1%, and 0% (unstretched) using the same processing parameters. The optical images show that the channel widths are 263.4, 78.5, and 26.3 μm, respectively, indicating that tensile strain enhances the effect of laser cutting. After fully releasing the strain to 0, the microchannel widths are characterized using scanning electron microscopy (SEM), and the widths are 7.3, 12.5, and 25.8 μm, respectively. This indicates that the greater the tensile strain applied to the material during processing, the tighter the microchannels close after release. The upper part of the microchannels cannot completely close due to material removal by laser.

To characterize the durability of the mode-switchable open microfluidic channels, a series of rigorous tests are conducted successively on the microchannels in protection mode, including sandpaper abrasion, tape peeling, twisting, and finger rubbing [Fig. 5(a) and supplementary Movie 3]. First, a 2000 mesh sandpaper is utilized to abrade the surface above the microchannels for 30 s, applying a force of 6 N. Second, transparent tape is placed over the microchannels, which are firmly adhered to the silicone membrane at a pressure of 10 N and subsequently peeled off, and the tape peeling process is repeated five times. Third, the silicone membrane is rigorously bent and twisted for 30 s, with this bending action being repeated five times. Finally, a finger is directly pressed on the microchannels with a pressure of 3 N, followed by 30 s of rubbing [Fig. 5(a)]. The morphology and cross-sectional profiles of the microchannels before and after the tests are recorded using CLSM [Figs. 5(b) and 5(c) and Fig. S8]. The results indicate that these tests only wear down the exposed silicone material without affecting the structure of the microchannels. After each test, the microchannel is stretched to working mode, and the water spreading time is recorded [Fig. 5(d)]. To avoid consumption of the hydrophilic coating, only one measurement is conducted in each test. The time required for water to flow through the whole channel (7.5 mm in length) increases from 1 to 3 s after twisting [Fig. 5(e)]. The results suggest that membrane twisting introduces friction between the channel walls, wearing the surface coating to some extent, yet the liquid mixing function remains preserved.

For a channel where each solid surface exhibits a uniform contact angle θ, the length of the air–liquid interface along the perimeter of the cross section is indicated as $L_{a\text{-}l}$, and the length of the liquid–solid interface is denoted as $L_{l\text{-}s}$. The condition for spontaneous capillary flow (SCF) is derived by Casavant *et al.*,[37,38]

$$\cos\theta > \frac{L_{a-l}}{L_{l-s}}. \quad (1)$$

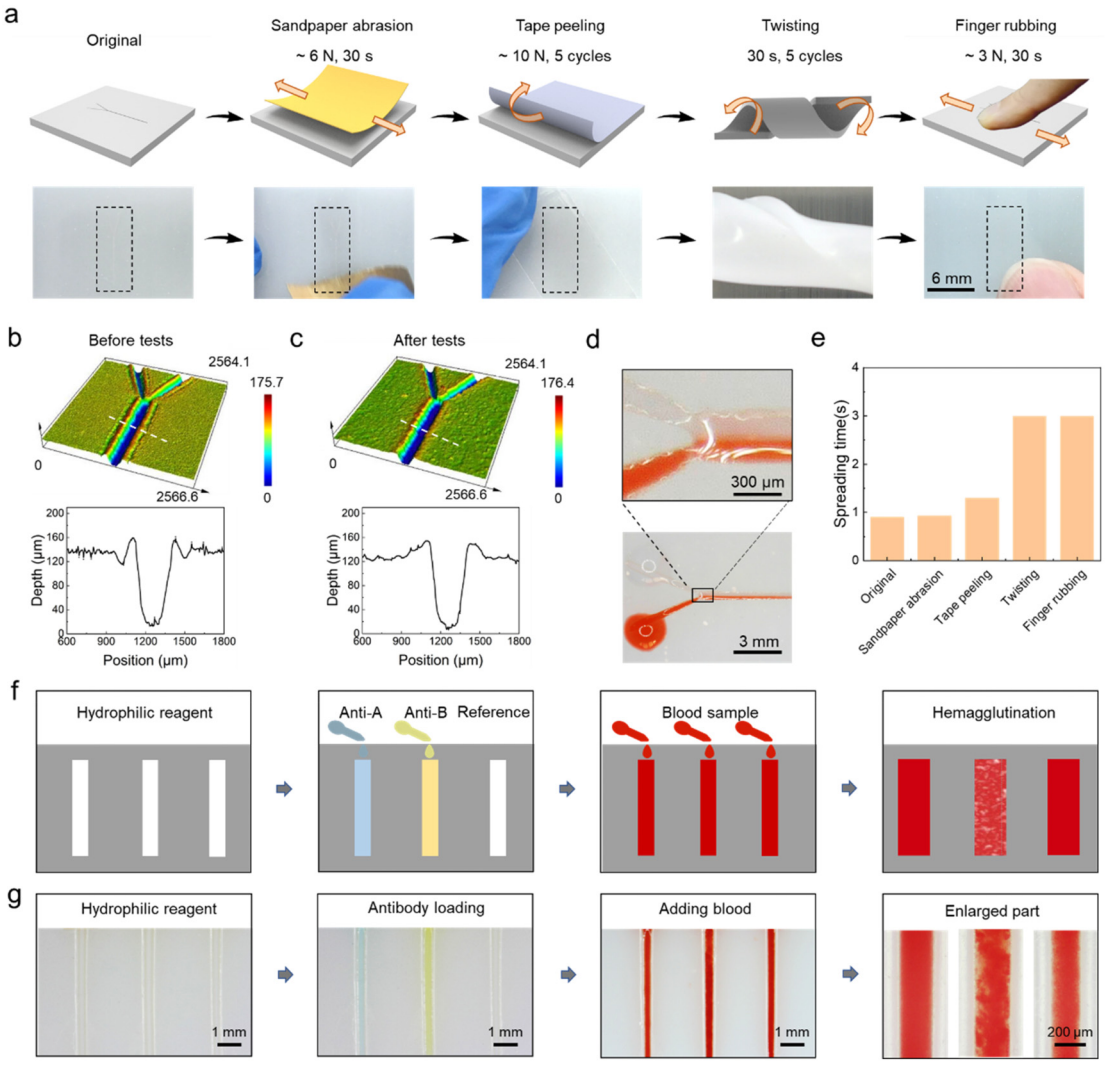

FIG. 5. Mechanical durability and blood typing analysis of mode-switchable open microchannels in harsh conditions. (a) Schematic and experimental images of tests including sandpaper abrasion, tape peeling, twisting, and finger rubbing. CLSM images and cross-sectional profiles of a Y-shaped channel before (b) and after (c) durability tests. (d) Demonstration of the fluid mixing function after a series of stringent tests. (e) Duration of water flow through the entire channel (7.5 mm in length) after each test. (f) Diagram illustrating the process of blood type analysis conducted in the stretched open microfluidic mode. (g) Actual blood type analysis process, and the blood type is B.

Here, the water contact angle on the hydrophilic reagent-modified laser-fabricated surface is 14.5° (Fig. S9). According to the cross-sectional profile, $L_{a\text{-}l}$ and $L_{l\text{-}s}$ are 325 and 440 μm, respectively; thus, the condition for SCF is satisfied. The water contact angle is determined by the surface microstructure and chemical coating.[39] During the rigorous test, both the microchannel structure and the hydrophilic coatings remain intact [Figs. 5(b) and 5(c)]; therefore, the condition for SCF is satisfied, and the liquid mixing function is maintained. Furthermore, the long-term chemical durability of the mode-switchable open microfluidic channels is investigated. The membranes with microchannels in the protected state are immersed in HCl solution (pH ~ 4), NaOH solution (pH ~ 10), and 5 wt. % NaCl solution for 10 days, respectively. The water spreading time along the main channel before and after the chemical immersion test is compared (Fig. S10). The results show that our microchannels, in the protective mode, maintain rapid fluid flow even after being soaked in alkaline and saline solutions for 10 days. The water spreading time increases from 0.52 to 1.73 s and from 0.38 to 1.48 s, respectively. However, after 10 days of soaking in acid, the fluid could still flow but at a reduced speed, with the water spreading time increasing from 0.8 to 5.8 s. This decrease in flow rate is likely due to partial dissolution of the coating by the acidic solution through the channel gaps (Fig. S7). In summary, the microchannels in the protective mode exhibit good chemical stability.

For blood banks and medical centers, precisely determining blood types is essential to ensure the safety of blood transfusions and transplants for patients. In remote outdoor areas, the environment for blood type testing can be harsh, with blood typing chips potentially subjected

to dust and wear. This exposure can lead to deterioration of the hydrophilic coating and contamination of the open microchannels. As a viable substitute, the durable open microfluidic channels presented here, featuring mode-switchable capability, offer a robust solution for reliable blood type tests. The blood type test capability of open microfluidic microchannels after the above-mentioned rigorous tests is investigated. The analysis of blood types is based on the principle of agglutination reactions.[40] Figure 5(f) and supplementary Movie 4 illustrate the operational procedure for blood type analysis. Initially, antibodies A and B (0.5 μl each) are added to the first two open microchannels, respectively, while the third microchannel is left without antibodies to serve as a reference. After 5 min, these antibodies are completely dried. Then, a drop of blood (0.5 μl) is introduced into each microchannel, where the spontaneous flow of blood facilitates its sufficient reaction with the antibody. Finally, the reaction phenomena are observed under a microscope. If the antibodies in the microchannels do not match the antigens carried by the red blood cells, no agglutination occurs, and red blood cells maintain a uniform distribution. Conversely, if agglutination occurs through antibody–antigen interactions, clusters of aggregated red blood cells form within the microchannels. For example, in the groove with anti-B antibody, clusters of aggregated cells indicate a B+ blood type, while no agglutination occurs in the groove with anti-A, showing a uniform distribution and consistent color; similarly, no agglutination occurs in the antibody-free channel [Fig. 5(g)]. The analysis results for other blood types can be obtained by similarly observing the distribution state of red blood cells in the separated channels. Representative blood type test results for the A+, AB+, and O+ blood types are shown in Fig. S11. The results indicate that open microfluidic channels with mode-switchable capability are effective for blood typing and exhibit excellent mechanical durability.

In summary, we introduce a bioinspired, demand-responsive mode-switchable strategy to enhance the mechanical durability of femtosecond laser-fabricated open microfluidic systems. This strategy enables the device to switch to a protective mode under harsh conditions or for long-term storage, achieved through simple release of the membrane. The stretched open microfluidic mode allows for capillary-driven liquid flow within a hydrophilic microchannel fabricated by a femtosecond laser. Upon encountering harsh conditions, the device transitions into a protective mode, effectively sealing the microchannels to prevent damage and contamination. This mode-switchable strategy ensures the device's resilience, allowing it to maintain spontaneous liquid flow even under rigorous testing conditions, including 2000 cycles of cotton swab rubbing, sand impact, sandpaper abrasion, tape peeling, twisting, and finger rubbing. As demonstrated through the practical application of blood type analysis, this mode-switchable open microfluidic device proves its exceptional mechanical durability and operational reliability under challenging conditions. The development and implementation of this mode-switchable mechanism provides opportunities in the field of microfluidics, broadening the potential applications of open microfluidic devices across a variety of real-world scenarios.

See the supplementary material for details on the experimental section and structural characterization.

This work was supported by the Key Research and Development Program of the Ministry of Science and Technology under Grant No. 2023YFB4604100 and the National Natural Science Foundation of China (No. 52105492). We acknowledge the Experimental Center of Engineering and Material Sciences at USTC for support with sample fabrication and characterization. This work was partially carried out at the USTC Center for Micro and Nanoscale Research and Fabrication, and we thank Yaping Li for her help on micro/nanofabrication.

AUTHOR DECLARATIONS

Conflict of Interest

The authors have no conflicts to disclose.

Author Contributions

Yahui Su: Conceptualization (equal); Resources (equal); Supervision (equal). **Linfeng Zheng:** Data curation (equal); Formal analysis (equal); Writing – original draft (equal). **Zhaoxin Lao:** Investigation (equal); Methodology (equal). **Zehang Cui:** Data curation (equal); Formal analysis (equal). **Chao Chen:** Formal analysis (equal); Methodology (equal). **Chenchu Zhang:** Data curation (equal); Formal analysis (equal). **Deng Pan:** Data curation (equal); Formal analysis (equal). **Yanlei Hu:** Methodology (equal); Writing – review & editing (equal). **Sizhu Wu:** Supervision (equal); Writing – review & editing (equal). **Yachao Zhang:** Conceptualization (equal); Funding acquisition (equal); Methodology (equal); Project administration (equal); Supervision (equal); Writing – original draft (equal); Writing – review & editing (equal). **Dong Wu:** Project administration (equal); Supervision (equal); Writing – review & editing (equal).

DATA AVAILABILITY

The data that support the findings of this study are available from the corresponding authors upon reasonable request.

REFERENCES

[1]S. Shrivastava, T. Q. Trung, and N.-E. Lee, "Recent progress, challenges, and prospects of fully integrated mobile and wearable point-of-care testing systems for self-testing," Chem. Soc. Rev. **49**(6), 1812–1866 (2020).
[2]C. Wang, M. Liu, Z. Wang, S. Li, Y. Deng, and N. He, "Point-of-care diagnostics for infectious diseases: From methods to devices," Nano Today **37**, 101092 (2021).
[3]M. Xiao, F. Tian, X. Liu, Q. Zhou, J. Pan, Z. Luo, M. Yang, and C. Yi, "Virus detection: From state-of-the-art laboratories to smartphone-based point-of-care testing," Adv. Sci. **9**(17), 2105904 (2022).
[4]J. Dinnes, P. Sharma, S. Berhane, S. S. van Wyk, N. Nyaaba, J. Domen, M. Taylor, J. Cunningham, C. Davenport, and S. Dittrich, "Rapid, point-of-care antigen tests for diagnosis of SARS-CoV-2 infection," Cochrane Database Syst. Rev. **2022**(7), Cd013705.
[5]Y. Shimakawa, G. Ndow, A. Kaneko, K. Aoyagi, M. Lemoine, Y. Tanaka, T. Cerceau, A. Ceesay, J. P. Vincent, and T. Watanabe, "Rapid point-of-care test for hepatitis B core-related antigen to diagnose high viral load in resource-limited settings," Clin. Gastroenterol. Hepatol. **21**(7), 1943–1946 (2023).
[6]J. Park, D. H. Han, and J.-K. Park, "Towards practical sample preparation in point-of-care testing: User-friendly microfluidic devices," Lab Chip **20**(7), 1191–1203 (2020).
[7]W. Jung, J. Han, J.-W. Choi, and C. H. Ahn, "Point-of-care testing (POCT) diagnostic systems using microfluidic lab-on-a-chip technologies," Microelectron. Eng. **132**, 46–57 (2015).
[8]B. Gao, Y. Yang, J. Liao, B. He, and H. Liu, "Bioinspired multistructured paper microfluidics for POCT," Lab Chip **19**(21), 3602–3608 (2019).
[9]S. Sachdeva, R. W. Davis, and A. K. Saha, "Microfluidic point-of-care testing: Commercial landscape and future directions," Front. Bioeng. Biotechnol. **8**, 602659 (2021).

[10]S.-M. Yang, S. Lv, W. Zhang, and Y. Cui, "Microfluidic point-of-care (POC) devices in early diagnosis: A review of opportunities and challenges," Sensors **22**(4), 1620 (2022).
[11]E. Berthier, A. M. Dostie, U. N. Lee, J. Berthier, and A. B. Theberge, "Open microfluidic capillary systems," Anal. Chem. **91**(14), 8739–8750 (2019).
[12]Q. Zhang, S. Feng, L. Lin, S. Mao, and J.-M. Lin, "Emerging open microfluidics for cell manipulation," Chem. Soc. Rev. **50**(9), 5333–5348 (2021).
[13]J. Yu, E. Berthier, A. Craig, T. E. de Groot, S. Sparks, P. N. Ingram, D. F. Jarrard, W. Huang, D. J. Beebe, and A. B. Theberge, "Reconfigurable open microfluidics for studying the spatiotemporal dynamics of paracrine signalling," Nat. Biomed. Eng. **3**(10), 830–841 (2019).
[14]Y. Si, C. Li, J. Hu, C. Zhang, and Z. Dong, "Bioinspired superwetting open microfluidics: From concepts, phenomena to applications," Adv. Funct. Mater. **33**(32), 2301017 (2023).
[15]S. Liu, Z. Zhan, Y. Si, C. Yu, L. Jiang, and Z. Dong, "Liquid shuttle mediated by microwick for open-air microfluidics," Adv. Funct. Mater. **33**(18), 2212485 (2023).
[16]H. Bai, X. Wang, Z. Li, H. Wen, Y. Yang, M. Li, and M. Cao, "Improved liquid collection on a dual-asymmetric superhydrophilic origami," Adv. Mater. **35**(17), 2211596 (2023).
[17]E. J. Walsh, A. Feuerborn, J. H. Wheeler, A. N. Tan, W. M. Durham, K. R. Foster, and P. R. Cook, "Microfluidics with fluid walls," Nat. Commun. **8**(1), 816 (2017).
[18]L. J. Barkal, A. B. Theberge, C.-J. Guo, J. Spraker, L. Rappert, J. Berthier, K. A. Brakke, C. C. Wang, D. J. Beebe, and N. P. Keller, "Microbial metabolomics in open microscale platforms," Nat. Commun. **7**(1), 10610 (2016).
[19]D. L. Giokas, G. Z. Tsogas, and A. G. Vlessidis, "Programming fluid transport in paper-based microfluidic devices using razor-crafted open channels," Anal. Chem. **86**(13), 6202–6207 (2014).
[20]M. M. Erenas, I. de Orbe-Paya, and L. F. Capitan-Vallvey, "Surface modified thread-based microfluidic analytical device for selective potassium analysis," Anal. Chem. **88**(10), 5331–5337 (2016).
[21]J. Berthier, K. Brakke, E. Furlani, I. Karampelas, V. Poher, D. Gosselin, M. Cubizolles, and P. Pouteau, "Whole blood spontaneous capillary flow in narrow V-groove microchannels," Sens. Actuators, B **206**, 258–267 (2015).
[22]B. Xu, T. Qin, J. Zhang, Y. Ding, Y. Su, J. Wu, D. Pan, Y. Zhang, and Z. Shen, "Cloth-based microfluidic analytical devices by laser-induced hydrophilization technique," Sens. Actuators, B **341**, 129998 (2021).
[23]A. W. Martinez, S. T. Phillips, and G. M. Whitesides, "Three-dimensional microfluidic devices fabricated in layered paper and tape," Proc. Natl. Acad. Sci. U. S. A. **105**(50), 19606–19611 (2008).
[24]P. Mostafalu, M. Akbari, K. A. Alberti, Q. Xu, A. Khademhosseini, and S. R. Sonkusale, "A toolkit of thread-based microfluidics, sensors, and electronics for 3D tissue embedding for medical diagnostics," Microsyst. Nanoeng. **2**(1), 16039 (2016).
[25]N. Maheshwari, A. Kottantharayil, M. Kumar, and S. Mukherji, "Long term hydrophilic coating on poly (dimethylsiloxane) substrates for microfluidic applications," Appl. Surf. Sci. **257**(2), 451–457 (2010).
[26]J. A. Callow and M. E. Callow, "Trends in the development of environmentally friendly fouling-resistant marine coatings," Nat. Commun. **2**(1), 244 (2011).
[27]B. Dai, K. Li, L. Shi, X. Wan, X. Liu, F. Zhang, L. Jiang, and S. Wang, "Bioinspired Janus textile with conical micropores for human body moisture and thermal management," Adv. Mater. **31**(41), 1904113 (2019).
[28]Y. Su, L. Chen, Y. Jiao, J. Zhang, C. Li, Y. Zhang, and Y. Zhang, "Hierarchical hydrophilic/hydrophobic/bumpy Janus membrane fabricated by femtosecond laser ablation for highly efficient fog harvesting," ACS Appl. Mater. Interfaces **13**(22), 26542–26550 (2021).
[29]K. Sugioka, J. Xu, D. Wu, Y. Hanada, Z. Wang, Y. Cheng, and K. Midorikawa, "Femtosecond laser 3D micromachining: A powerful tool for the fabrication of microfluidic, optofluidic, and electrofluidic devices based on glass," Lab Chip **14**(18), 3447–3458 (2014).
[30]Y. Lu, Y. F. Li, G. Wang, Y. Yu, Z. Bai, Y. Wang, and Z. Lu, "Femtosecond laser fabrication of microchannels in transparent hard materials," Adv. Mater. Technol. **8**(14), 2300015 (2023).
[31]Z. Lin and M. Hong, "Femtosecond laser precision engineering: From micron, submicron, to nanoscale," Ultrafast Sci. **2021**, 9783514.
[32]X. Li, G. Yuan, W. Yu, J. Xing, Y. Zou, C. Zhao, W. Kong, Z. Yu, and C. Guo, "A self-driven microfluidic surface-enhanced Raman scattering device for Hg^{2+} detection fabricated by femtosecond laser," Lab Chip **20**(2), 414–423 (2020).
[33]J. Yong, Q. Yang, J. Huo, X. Hou, and F. Chen, "Underwater gas self-transportation along femtosecond laser-written open superhydrophobic surface microchannels (<100 μm) for bubble/gas manipulation," Int. J. Extreme Manuf. **4**(1), 015002 (2022).
[34]K. S. Dogbevi, B. K. D. Ngo, C. W. Blake, M. A. Grunlan, and G. L. Coté, "Pumpless, 'self-driven' microfluidic channels with controlled blood flow using an amphiphilic silicone," ACS Appl. Polym. Mater. **2**(4), 1731–1738 (2020).
[35]R. Su, J. Wen, Q. Su, M. S. Wiederoder, S. J. Koester, J. R. Uzarski, and M. C. McAlpine, "3D printed self-supporting elastomeric structures for multifunctional microfluidics," Sci. Adv. **6**(41), eabc9846 (2020).
[36]Z. Cui, Y. Zhang, Z. Zhang, B. Liu, Y. Chen, H. Wu, Y. Zhang, Z. Cheng, G. Li, and J. Yong, "Durable Janus membrane with on-demand mode switching fabricated by femtosecond laser," Nat. Commun. **15**(1), 1443 (2024).
[37]B. P. Casavant, E. Berthier, A. B. Theberge, J. Berthier, S. I. Montanez-Sauri, L. L. Bischel, K. Brakke, C. J. Hedman, W. Bushman, and N. P. Keller, "Suspended microfluidics," Proc. Natl. Acad. Sci. U. S. A. **110**(25), 10111–10116 (2013).
[38]J. Berthier, K. A. Brakke, and E. Berthier, "A general condition for spontaneous capillary flow in uniform cross-section microchannels," Microfluid. Nanofluid. **16**, 779–785 (2014).
[39]R. N. Wenzel, "Resistance of solid surfaces to wetting by water," Ind. Eng. Chem. **28**(8), 988–994 (1936).
[40]M. Li, J. Tian, M. Al-Tamimi, and W. Shen, "Paper-based blood typing device that reports patient's blood type 'in writing'," Angew. Chem. **124**(22), 5593–5597 (2012).